Journal of Cell Science 106, 941-953 (1993)
Printed in Great Britain © The Company of Biologists Limited 1993

HIV-induced syncytia of a T cell line form single giant pseudopods and are motile

Andrew Sylwester[1], Deborah Wessels[1], Stephanie A. Anderson[2], Ronald Q. Warren[2], Damon C. Shutt[1], Ronald C. Kennedy[2] and David R. Soll[1,*]

[1]Department of Biological Sciences, University of Iowa, Iowa City, IA 52242, USA
[2]Center for AIDS Research, Southwest Foundation for Biomedical Research, San Antonio, TX 78228, USA

*Author for correspondence

SUMMARY

The human immunodeficiency virus, HIV, induces syncytium formation in cultures of many T cell lines. These syncytia have previously been viewed as disorganized fusion products in the throes of death. Evidence is presented that in HIV1-infected SupT1 cultures, syncytia five times to over one hundred times larger than single cells organize their many nuclei into blastula-like balls, reorganize their cytoskeleton to mimic that of a single cell, and extend single, giant pseudopods in a polar fashion. Medium-sized syncytia are capable of translocation through extension of these giant pseudopods. The rate of translocation of syncytia is comparable to that of single cells. Single cell motility, syncytium motility and pseudopod extension also appear to play roles in the recruitment of cells into syncytia. Finally, condensation of F-actin at cell-syncytium and syncytium-syncytium adhesion sites suggests the involvement of the cytoskeleton in the adhesion and/or subsequent fusion event. These results suggest that the fusion events involved in HIV-induced syncytia formation involve both cell motility and reorganization of the cytoskeleton, and demonstrate that syncytia are highly organized, motile entities.

Key words: HIV, syncytia, T cell, motility, actin

INTRODUCTION

Infection with the human immunodeficiency virus (HIV) eventually leads to a drastic reduction in the level of CD4-positive T lymphocytes (Lane et al., 1975; Fauci, 1988). The direct cytopathic effects of HIV can be studied in vitro in T cell lines, where infection sometimes results in the genesis of multicellular fusion products, referred to as syncytia, which eventually lyse (Lifson et al., 1986b; Sodroski et al., 1986). However, there has been little attention paid to the roles of T cell motility, morphology and the cytoskeleton in HIV-induced syncytium formation. This may be due in part to the lack of attention that has been paid to the motility of uninfected CD4-positive T cells, and in part to the view that HIV-induced fusion leads to cellular disorganization, which in turn leads to lysis (Lifson et al., 1986b).

We have, therefore, examined the role of cell motility in syncytium formation, the changes in cytoskeletal organization and morphology accompanying syncytium formation, and the motile behavior of syncytia in HIV-infected cultures of the T cell line SupT1. Results are presented that demonstrate that the majority of cells in uninfected and HIV-infected T cell lines are motile and translocate through extension of single anterior pseudopods. In contrast to the view that syncytia are giant disorganized monstrosities in the throes of death, we present evidence that syncytia can in fact be highly organized multinuclear giants, which exhibit the equivalent of single cell organization and polarity, translocate at rates comparable to single cells through the extension of giant pseudopods many times the size of a single cell, can actively recruit single cells for subsequent fusion, and fuse among themselves prior to lysis.

MATERIALS AND METHODS

Cells and virus

Clones of the human CD4-positive T cell line SupT1 were prepared in soft agar and passed in liquid medium by described methods (Smith et al., 1984). The SupT1 cell line was established in vitro from a patient with a T cell malignancy consistent with non-Hodgkin's lymphoma (Smith et al., 1984). The HIV-1 IIIB isolate was kindly provided by Dr Robert Gallo. The virus was passed in the MOLT-3 human CD4-positive T cell line. The SupT1 cell line was maintained in RPMI 1640 medium supplemented with 25 mM HEPES buffer, a 1:100 dilution of MEM nonessential amino acid solution #M-7145 (Sigma, St. Louis), 10% heat-inactivated fetal calf serum, 2 mM L-glutamine, 1 mM sodium pyruvate, 100 units per ml of penicillin and 100 μg per ml of streptomycin.

HIV-1 induced syncytium formation

To induce syncytium formation, 1 ml of supernatant fluid from an infected MOLT-3 cell culture, which contained approximately

5000 tissue culture infectious dose 50 ($TCID_{50}$), was added to a pellet of 10^7 SupT1 cells. After 2 hours, the pellet was diluted to 10^6 cells per ml in tissue culture flasks. Flasks were incubated in 5% CO_2 at 37°C. Mock infected SupT1 cells were similarly prepared without addition of HIV-1.

Fluorescent staining

Cultures were gently mixed and aliquots pipetted onto 12 mm round glass coverslips previously treated with a poly-L-lysine solution (P-8920) purchased from Sigma, St. Louis. Coverslips were incubated in 5% CO_2 at 37°C for 30 minutes to allow cells to settle. For F-actin, tubulin, and DNA staining, coverslips were drained and preparations fixed in 2% glutaraldehyde plus 0.5% Triton X-100 in RPMI medium at 2°C for 5 minutes. Preparations were then rinsed two times with RPMI medium, one time with a 1:1 solution of RPMI and PBS (138 mM NaCl, 2.5 mM KCl, 10 mM Na_2HPO_4 and 1.8 mM KH_2PO_4), and 3 times with PBS. Autofluorescence was quenched by treating coverslips with 5 mg per ml of $NaBH_4$ in PBS for 15 minutes, followed by 3 rinses with PBS. For F-actin and DNA localization, preparations were then stained with either a solution containing 10 units per ml of FITC-conjugated phalloidin (Molecular Probes, Eugene, OR) in PBS for 15 minutes at room temperature for F-actin, or with 100 μg per ml DAPI (Molecular Probes, Eugene, OR) in PBS for DNA staining, respectively. Coverslips were then rinsed 3 times with PBS and mounted onto microscope slides with Vectashield mounting medium (Vector Labs, Burlingham, CA). Preparations were examined and photographed through a Zeiss ICM 405 inverted microscope equipped for epifluorescent microscopy with a 100 W super pressure mercury lamp or with a Bio-Rad 600 MRC confocal microscope.

For tubulin staining, fixed preparations were blocked for 1 hour at 4°C with PBS plus 5% BSA and then exposed to 25 μl of undiluted antitubulin monoclonal antibody E7 obtained from the Developmental Studies Hybridoma Bank at the University of Iowa under contract from the NICHD. Coverslips were rinsed 3 times in PBS containing 5% BSA and 0.02% NaN_3. After the final rinse, coverslips were incubated for 20 minutes at room temperature in 25 μl of FITC-conjugated goat $F(ab)_2$ fragment to mouse IgG (whole molecule, no. 55504; Cappel Res. Prod., Durham, NC) diluted 1:200 in PBS plus 5% BSA. Coverslips were rinsed 2 times in PBS plus 5% BSA, once in PBS, and mounted in 20 μl Vectashield.

Scanning electron microscopy

Preparations were fixed according to the method described for phalloidin and DAPI staining, except Triton X-100 was omitted from the fix, then treated with a 1% solution of O_sO_4 in 50% PBS for 15 minutes at room temperature. Preparations were rinsed 3 times in PBS, 1 time in a 1:1 solution of PBS and double distilled water, 1 time in double distilled water alone, and then passed through an ethanol dehydration sequence (15,35,50,75,85,95,100%). Ethanol was then substituted with HMDS (Electron Microscopy Sciences, Fort Washington, PA), and after 4 changes of HMDS, coverslips were air-dryed. Preparations were then sputter-coated with gold-platinum and imaged with a 10 kV accelerating voltage on a Hitachi S-4000 scanning electron microscope.

Behavioral analysis

Cell and syncytium behavior was monitored by general methods previously described in detail (Soll, 1988; Soll et al., 1988; Wessels and Soll, 1990; Titus et al., 1993). In brief, a culture flask with a settled suspension of uninfected or infected cells was positioned on the stage of a Zeiss ICM405 inverted microscope equipped with a long distance condenser and low numerical aperture phase-contrast and bright-field objectives. Culture temperature was maintained at 37°C±1°C by means of a thermostatically-controlled air curtain. Cultures were continuously videorecorded on 3/4 inch video tape through a newvicon 2400-07 video camera (Hamamatsu Photonics K.K., Hamamatsu City, Japan). Digitization was performed with the manual information retrieval option in the DIAS software package (Solltech Inc., Iowa City, IA), which represents the advanced version of the DMS software package (Soll, 1988; Soll et al., 1988) in a Quadra 900 computer (Apple Computers, Cupertino, CA). Cell and syncytium perimeters were digitized at 15 second intervals and motion parameters computed through the DIAS program. 'Instantaneous velocity' was computed by the central difference method (Maron, 1982). 'Difference pictures' were generated by superimposing the images of 2 frames separated by a prescribed interval. Regions in the later image not overlapping the earlier image were considered 'expansion' zones and were filled; regions in the earlier image not overlapping the later image were considered 'contraction' zones and were hatched; and regions common to both images were unfilled (Soll, 1988; Soll et al., 1988). The 'roundness' parameter was computed as $[(4P\times\text{area})/\text{perimeter}^2]\times 100$. 'Directional change' at frame $n+1$ was computed as the absolute difference in degrees, of the translocation vector between frames $n-1$ and n, and frames n and $n+1$. 'Positive flow' was computed as the percent of cell area in expansion zones for an individual difference picture (Soll, 1988; Soll et al, 1988).

RESULTS

Uninfected SupT1 cell morphology and ultrastructure

After 48 hours in culture, SupT1 cells were distributed either individually or in aggregates on the culture flask substratum (Fig. 1A,B). In either case, the majority of cells exhibited morphological asymmetry, with a main round cell body and single extended pseudopod (Fig. 1A,B). In a minority of cases, cell bodies were more elongate. In Fig. 2A through D, scanning electron micrographs are presented of four representative Sup T1 cells. The main body of each Sup T1 cell was round, with a single thin pseudopod possessing folds and in some cases short filopodial projections. The pseudopod was usually flat on the substratum (Fig. 2A through D). Uninfected SupT1 cells, which had entered aggregates, maintained the same morphology as independent cells, with a round cell body and a single thin, sometimes wavy, pseudopod (Fig. 2E,F).

DAPI staining of DNA demonstrated that a large, round, lobed nucleus filled most of the space in the main body of uninfected SupT1 cells (Fig. 3A through D). In a minority of cells, which exhibited a more elongate shape, the nucleus was also more elongate, but still filled most of the space of the main cell body.

Phalloidin was used to stain F-actin. Staining was observed just under the plasma membrane of the main cell body and pseudopod (arrow) when viewed by confocal microscopy (Fig. 3E,F). Pseudopods stained more intensely than the outer cortex of the main cell body, and this was evident when stained cells were viewed by epifluorescent microscopy (Fig. 3G,H). Each cell body also contained a cluster of stained particles, most evident in confocal micrographs (arrowhead, Fig. 3F).

Microtubules were visualized by indirect immunofluo-

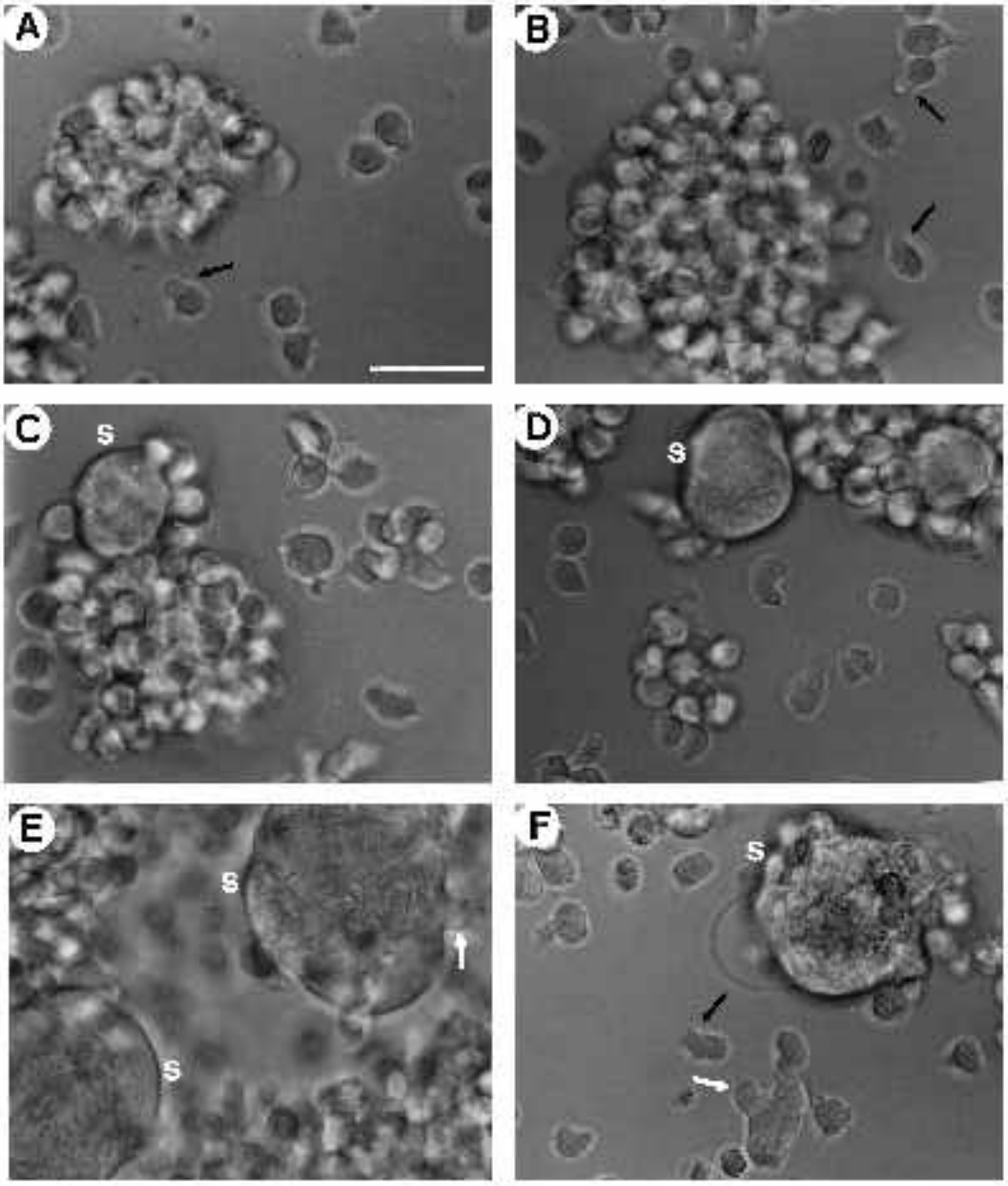

Fig. 1. Phase-contrast micrographs of fields of SupT1 cells in culture. (A,B) uninfected cultures exhibiting aggregates as well as individual cells. (C,D) HIV-treated cultures after 48 hours exhibiting syncytia, aggregates and individual cells. (E,F) HIV-treated cultures after 72 hours exhibiting syncytia, aggregates and individual cells. The black arrows in (A) and (B) point to examples of individual cells with visible pseudopods; the white arrow in (E) points to a pseudopod extending from a giant syncytium, and the white arrow in (F) points to a pseudopod extending from a small syncytium; S denotes medium and large-sized syncytia. Note the majority of individual cells in all panels have motile-like morphologies. Bar in (A), 48 μm.

rescence with an antiserum to tubulin. Neither the antiserum nor the fluorescence-tagged secondary antibody alone stained cells. The anti-tubulin reagent stained a microtubule array emanating from a single microtubule organizer usually located close to the supporting substratum and just under the cell nucleus (arrows, Fig. 3I). Since the lobed nucleus of each SupT1 cell filled most of the cell body (Fig. 3B,D), the microtubule array was restricted to the cytoplasmic cortex. Therefore, confocal sections through the cytoplasmic cortex at the top of the cell (Fig. 3J) contained a continuous meshwork of tubules, but confocal sections through the center of the cell (Fig. 3K) contained a stained cortical ring and an unstained nuclear center. Microtubules were also observed penetrating pseudopods (Fig. 3L).

Motile behavior of uninfected SupT1 cells

The majority of more than 100 randomly selected, individual SupT1 cells underwent shape changes, and more than half extended pseudopods during a 10 minute period of analysis. However, only half of these latter cells translocated in a persistent fashion along the plastic substratum due to weak adhesion. The cell bodies of several individual cells that formed pseudopods were not sufficiently attached to the substratum, and when the pseudopod extended, they actually pushed the cell bodies backwards. To analyze the motile behavior of SupT1 cells, 11 individual cells that exhibited anterior translocation (30% of 110 cells analyzed) were videorecorded for periods ranging from 7.5 to 20 minutes and their perimeters were digitized into the DIAS data base using the manual framegrabber data acquisition option (see Materials and Methods). Perimeters were digitized at 15 second intervals. The average instantaneous velocity of individual SupT1 cells was 6.6±1.8 μm per min and the range was 4.5 to 9.7 μm per

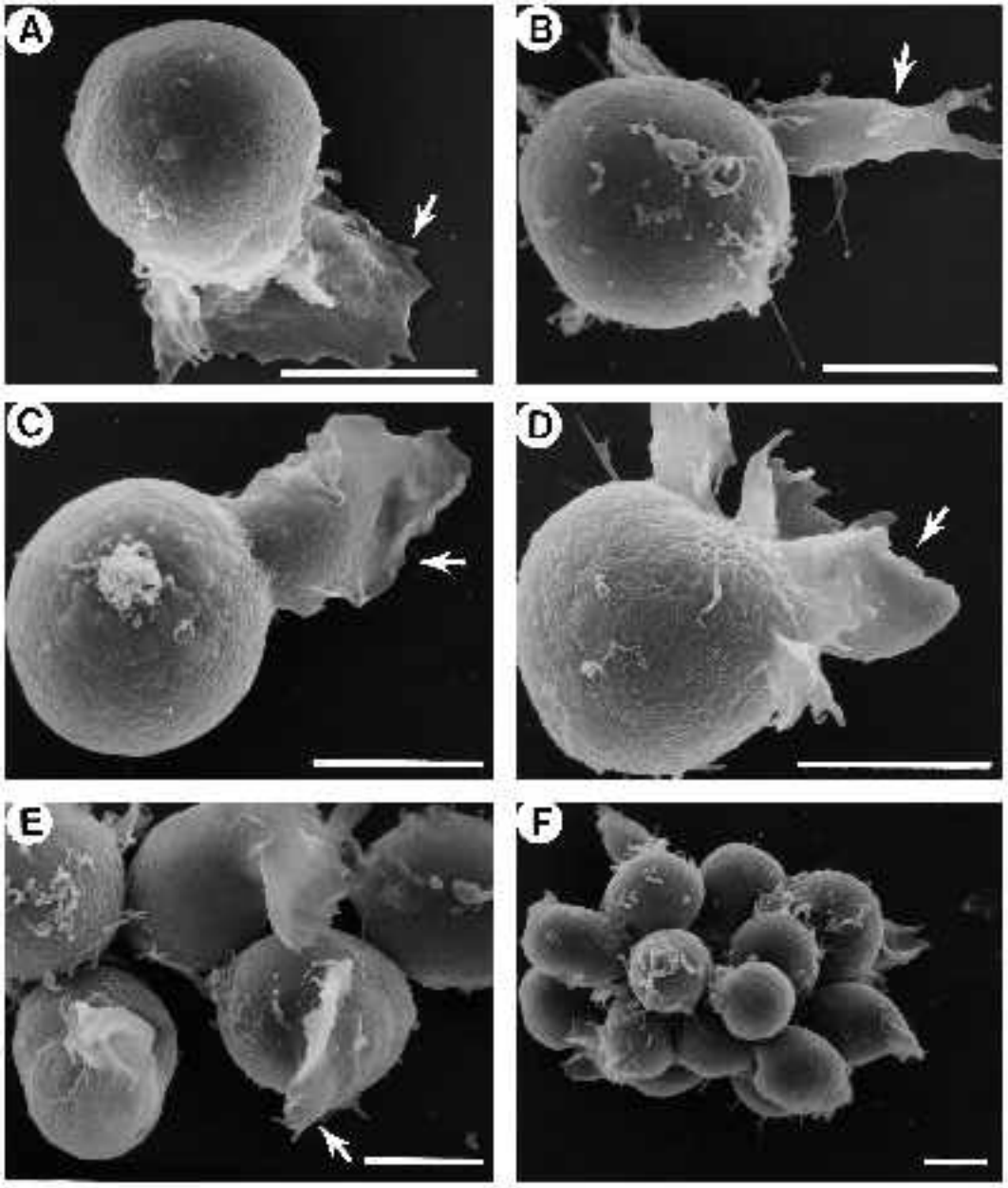

Fig. 2. Scanning electron micrographs of uninfected SupT1 cells. (A through D) individual cells, (E,F) aggregated cells. Note that both individual and aggregated cells exhibit a relatively round cell body and a single thin pseudopod noted by a white arrow. Bars, 5 μm.

min (Table 1). The persistence of cellular translocation was measured by the directional change parameter. If a cell is moving directly forward, this parameter would average 0 deg per 15 seconds, and if a cell was moving randomly or turning at right angles every 15 minute, this parameter would average 90 deg per 15 min. The directional change parameter averaged 43.3±9.8 deg per 15 min, demonstrating an anterior bias for translocation. The directionality and persistence of translocation is best assessed by examining the tracks of individual cells. In Fig. 4A and B, perimeter and centroid tracks are presented, respectively, for 3 representative SupT1 cells. In each case, the cell exhibited long linear tracks with little lateral deviation. Directionality is also demonstrated in difference pictures, which provide a 2-dimensional view of cellular extension and contraction during translocation (see Materials and Methods). In Fig. 4C and D, difference pictures have been generated during 120 second periods for cells 1 and 2, respectively, in Fig. 4A and B. In each case, it is evident that (1) the cell is undergoing continuous shape changes, (2) that expansion (filled) and contraction (hatched) zones occur in a polar, or directional, fashion, and (3) that the vectors drawn between the centroid of the earlier image (small open circle) and the centroid of the later image (dot) in the majority of difference pictures point in the same general direction.

Single cell morphology, ultrastructure and behavior in HIV-1 infected cultures

Under the conditions employed, cells in HIV-1 infected SupT1 cultures were distributed individually or in aggregates at 24 hours post-infection, in a fashion similar to uninfected cultures. However, after 48 hours, infected cultures differed from uninfected cultures by the appearance of giant cells, or small syncytia (Fig. 1C,D). After 72 hours,

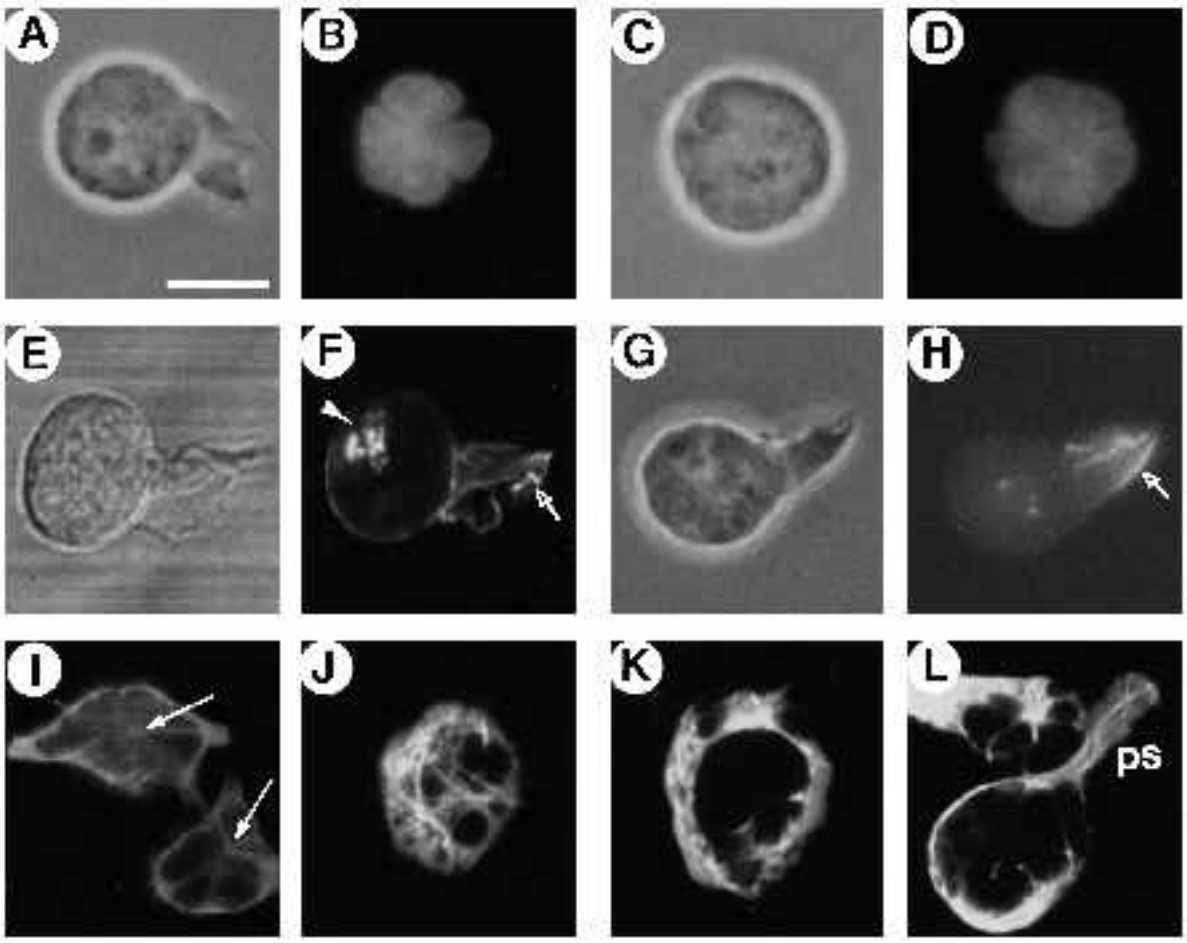

Fig. 3. Nucleus, F-actin and microtubule localization in uninfected SupT1 cells. (A,C and B,D) Phase-contrast and epifluorescent images, respectively, of DAPI-stained cells (note how the lobed nucleus fills most of the cell body). (E,F) Phase-contrast and confocal fluorescent images, respectively, of FITC-phalloidin-stained cells (note staining in cortex of cell, in cortex of pseudopod noted by arrow, and vesicle-like structures in a cluster, noted with arrow head). (G,H) Phase-contrast and epifluorescent micrographs, respectively, of a cell stained with phalloidin (note intense staining in pseudopod). (I) Epifluorescent micrograph of cell stained with antiserum to tubulin and visualized close to the substratum (note the microtubule organizer at the center of each cell image noted by an arrow). (J) confocal section through the cortex of the upper surface of a cell stained for tubulin. (K) confocal section through the center of a cell stained for tubulin. (L) confocal section through the cell body and an elongate pseudopod (p.s.) of a cell stained for tubulin. Bar in (A), 10 μm.

Table 1. Motility and area parameters of individual SupT1 cells and syncytia

	Individual cells	Syncytia
No. cells analyzed	11	11
Av. time of analysis	12.5±3.4 min (7.5-20.0 min)	12.9±6.5 min (4.75-19.75 min)
Av. instantaneous vel.	6.6±1.8 μm/min (4.5-9.7 μm/min)	8.7±1.9 μm/min (6.3-11.7 μm/min)
Av. area	179.0±34.0 μm^2 (119-239 μm^2)	1918±1926 μm^2 (596-7285 μm^2)
Av. maximum length	20.6±2.4 μm (16.5-24.0 μm)	57.6±20.8 μm (37.3-107 μm)
Av. roundness	72.3±6.5% (61.4-85.1%)	72.0±10.8% (60.8-93.6%)
Av. positive flow	21.1±3.7%/15 s (17.1-28.5%/15 s)	12.8±4.7%/15 s (3.8-20.0%/15 s)
Directional change	43.7±7.6 deg/15 s (28.6-54.4 deg/15 s)	43.3±9.8 deg/15 s (35.9-60.6 deg/15 s)

Parameters were computed for individual cells and syncytia at 15 second intervals.

extremely large syncytia, usually with single cells adhering to their perimeter, were evident throughout the culture (Fig. 1E,F).

Individual SupT1 cells in 48-hour infected cultures were examined for morphology, cytoskeletal organization and ultrastructure. To be sure that these cells were not influenced by syncytia, cells were analyzed only if they were positioned 6 cell lengths or greater from any syncytium. The morphologies (Fig. 1C,D), ultrastructural organization and motile behavior of these individual cells were similar to those of parallel uninfected cultures incubated for similar lengths of time and described here in preceding sections.

Syncytium morphology and cytoskeletal organization

Most small, medium sized and large syncytia were relatively round. However, the majority of syncytia in all size classes were behaviorally active, extending both small and extremely large pseudopods along or above the substratum noted by unfilled arrows in Fig. 1E,F. When viewed by

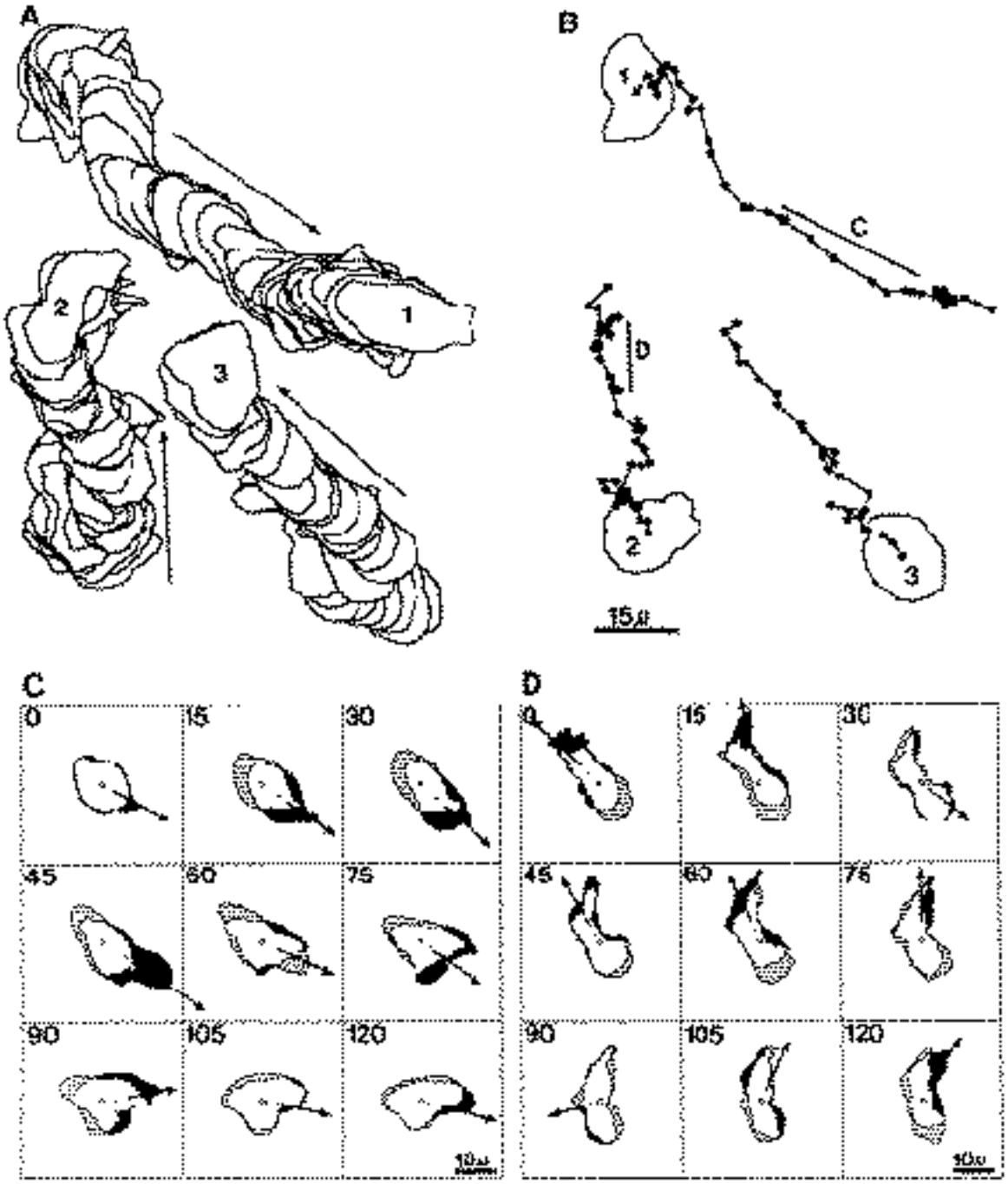

Fig. 4. Motility of SupT1 cells. SupT1 cells were videorecorded and digitized into the DIAS data file. Tracks of cell perimeters (A) and cell centroids (B) were then computer generated and plotted at 15 second intervals. Arrows point in the direction of translocation for the cells in (A). The cell perimeter is presented at zero time in the centroid plots in (B). Difference pictures were generated for cell 1 (C) and cell 2 (D) in which expansion zones are filled, contraction zones are hatched and common zones are unfilled (see Materials and Methods for description of a difference picture). The interval between the 2 images in each difference picture was 15 seconds. The direction of translocation is noted by an arrow in each difference picture. The periods during which the difference pictures were generated are diagrammed as lines in (B). μ represents μm.

scanning electron microscopy, most syncytia exhibited a single, large, polar pseudopod (noted by large filled white arrows in Fig. 5A,C,D,E). These extensions were similar in morphology to the single pseudopods of unfused individual cells of uninfected or infected cultures, but usually many times larger (compare pseudopods of syncytia with pseudopods of single cells in Fig. 5E). The main synctium body possessed large numbers of fibers at the deduced posterior end attached to the substratum noted by arrowheads in Fig. 5C,D,E. In addition, mottled round protrusions slightly smaller than single cells were often visible on syncytia (Fig. 5C) and might represent carcasses of single cell

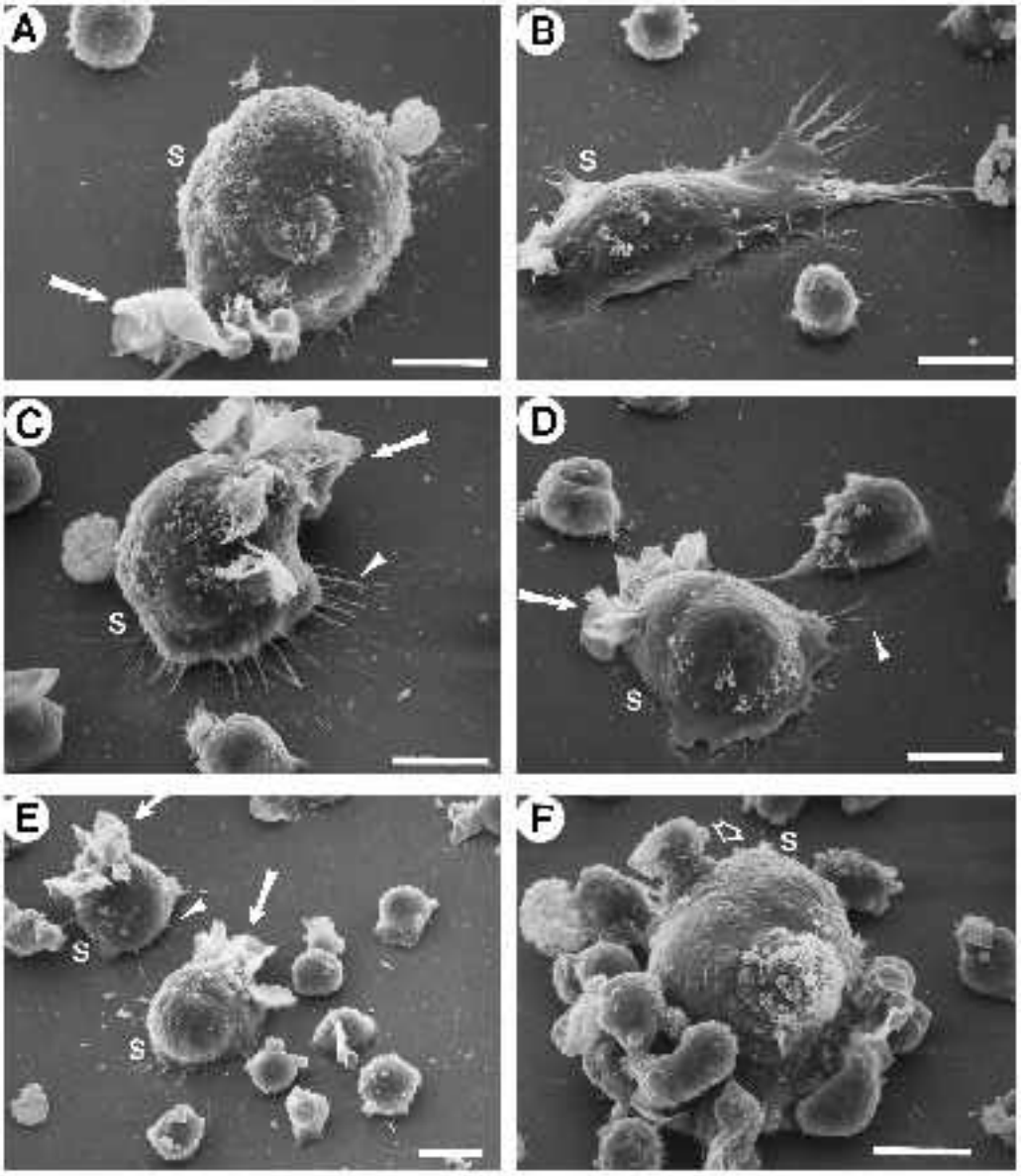

Fig. 5. Scanning electron micrographs of syncytia (S) with surrounding individual cells. Note that each syncytium in (A) through (E) possesses a very large visible pseudopod noted by an arrow. The relative size of each syncytium and its pseudopod can be assessed by comparison with the single cells in its immediate vicinity. The syncytium in (F) is covered with single cells and a possible fusion event on the syncytium perimeter is noted by an unfilled arrow. Note extension of the syncytium towards the single cell body. Arrowheads point to posterior fibers. Bars, 10 μm.

fusants not incorporated into the main syncytium contour. A possible fusion of a single cell and large syncytium is indicated by an unfilled arrow in Fig. 5F. Note the localized extension of the syncytium towards the fusing individual cell.

The extension of a single large pseudopod suggested that syncytia were capable of generating polarity similar to that of a single cell and therefore were capable of subcellular organization. An analysis of the organization of nuclei and the cytoskeleton of syncytia supported this suggestion. DAPI staining demonstrated that the multiple nuclei in medium sized syncytia were organized into blastula-like complexes with central, nuclear-free cores (Fig. 6B,D). In very large syncytia, multiple nuclear complexes were evident (Fig. 6J), suggesting that smaller syncytia had fused and the nuclear complexes of these smaller syncytia maintained their integrity after fusion. In spite of apparent syncytium-syncytium fusion, many of the giant syncytia still formed dominant large pseudopods several times the size of a single cell (Fig. 6I). Confocal sections of phalloidin-stained syncytia demonstrated that the cores of the blastula-like nuclear complexes were enriched with F-actin (noted by dark arrows in Fig. 7A through D). In addition, F-actin was localized in internuclear regions and just under the plasma membrane of the main cell bodies and pseudopods. Close examination of the dense F-actin core of the blastula-like nuclear complexes revealed punctate or vesicle-like staining (most notable in Fig. 7A). Indirect immunofluorescent staining of tubulin revealed a microtubule mesh covering the outer surface of the blastula-like multinuclear complexes. In Fig. 6F,H fluorescent micrographs are presented of small syncytia stained for tubulin and photographed in a focal plane at the dorsal surface where the microtubule array in the syncytial cortex was visible.

Syncytia are motile

The majority of 50 syncytia underwent shape changes and

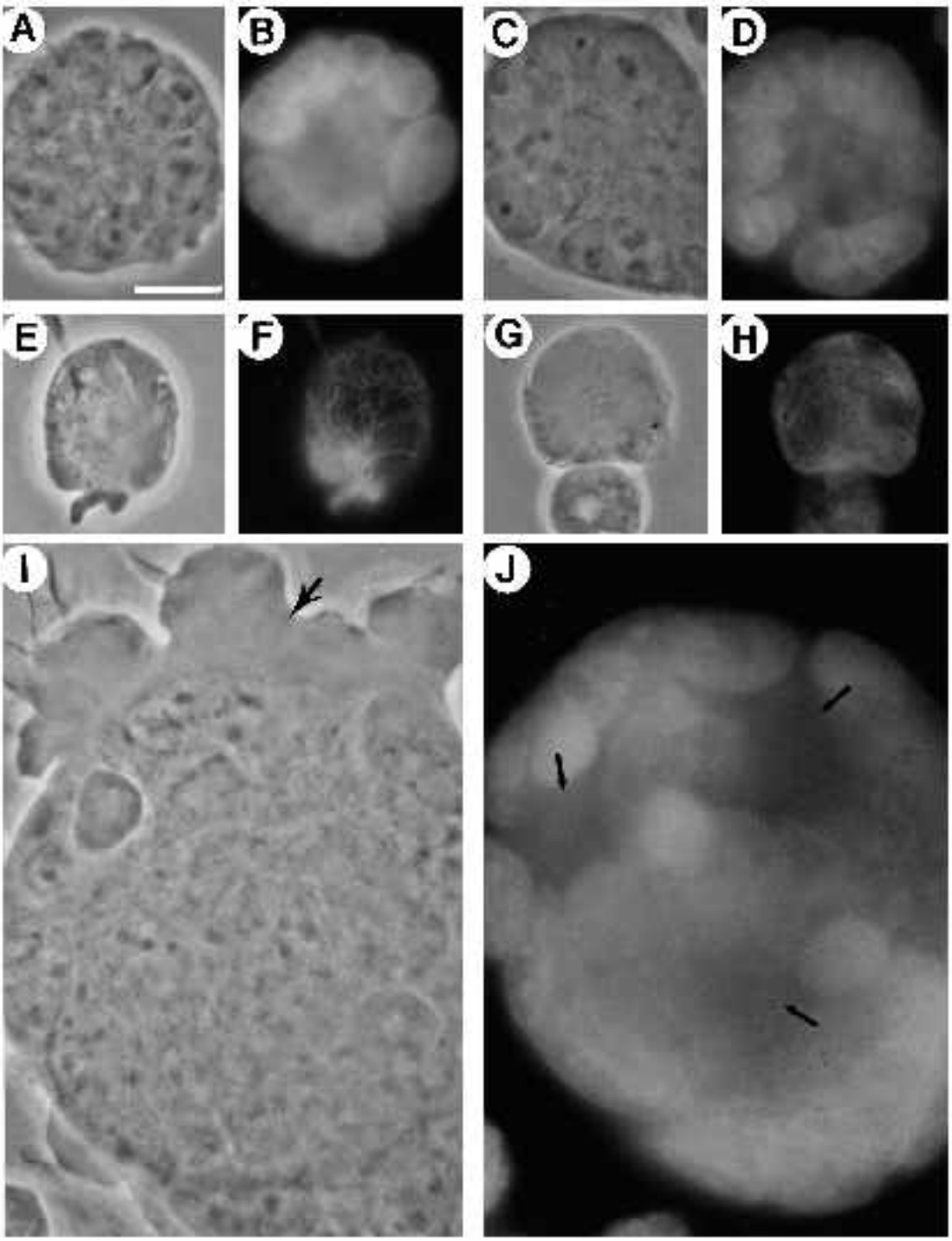

Fig. 6. Nuclear and microtubule distributions in syncytia. (A,C and B,D) Phase-contrast and epifluorescent images, respectively, of medium-sized syncytia stained with DAPI (note the blastula-like distribution of nuclei and hollow core). (E,G and F,H) Phase-contrast and epifluorescent images, respectively, of two small syncytia stained with antiserum to tubulin and photographed at a focal plane at the dorsal surface of the syncytium. (I,J) Phase-contrast and epifluorescent micrographs of a very large syncytium stained with DAPI (note the single large pseudopodium at one end of the syncytium pointed to by an arrow in (I), and the multiple nuclear complexes with empty cores in (J), noted by arrows). Bar in (A), 10 μm.

more than half extended pseudopods during a 10 minute period of analysis, and one third translocated on the plastic substratum. Eleven translocating syncytia were videorecorded for periods ranging from 4.75 to 19.75 minutes, and their perimeters digitized into the DIAS data base at 15 second intervals. Although the average area of the analyzed syncytia was 1918±1926 μm^2, roughly 10 times the average area of T cells, the average instantaneous velocity was 8.7±1.9 μm per minute, just slightly greater than that measured for individual T cells (Table 1). Average positive flow, measured as the percentage of the cell area encompassed in expansion zones generated from difference pictures at 15 second intervals, was 12.8±4.7% per 15 seconds, roughly half as great as that of individual cells. However, since the area of a syncytium was roughly 15 times that of a cell in this analysis, the actual expansion in areas of syncytia was, on average, 6 times greater than that of a single cell. The average directional change parameter of syncytia was 43.3±9.8 deg/15 s, almost identical to that of translocating SupT1 cells (Table 1). Therefore, syncytia moved not only at roughly the same rate, but with the same directionality as individual cells. Both the directionality and

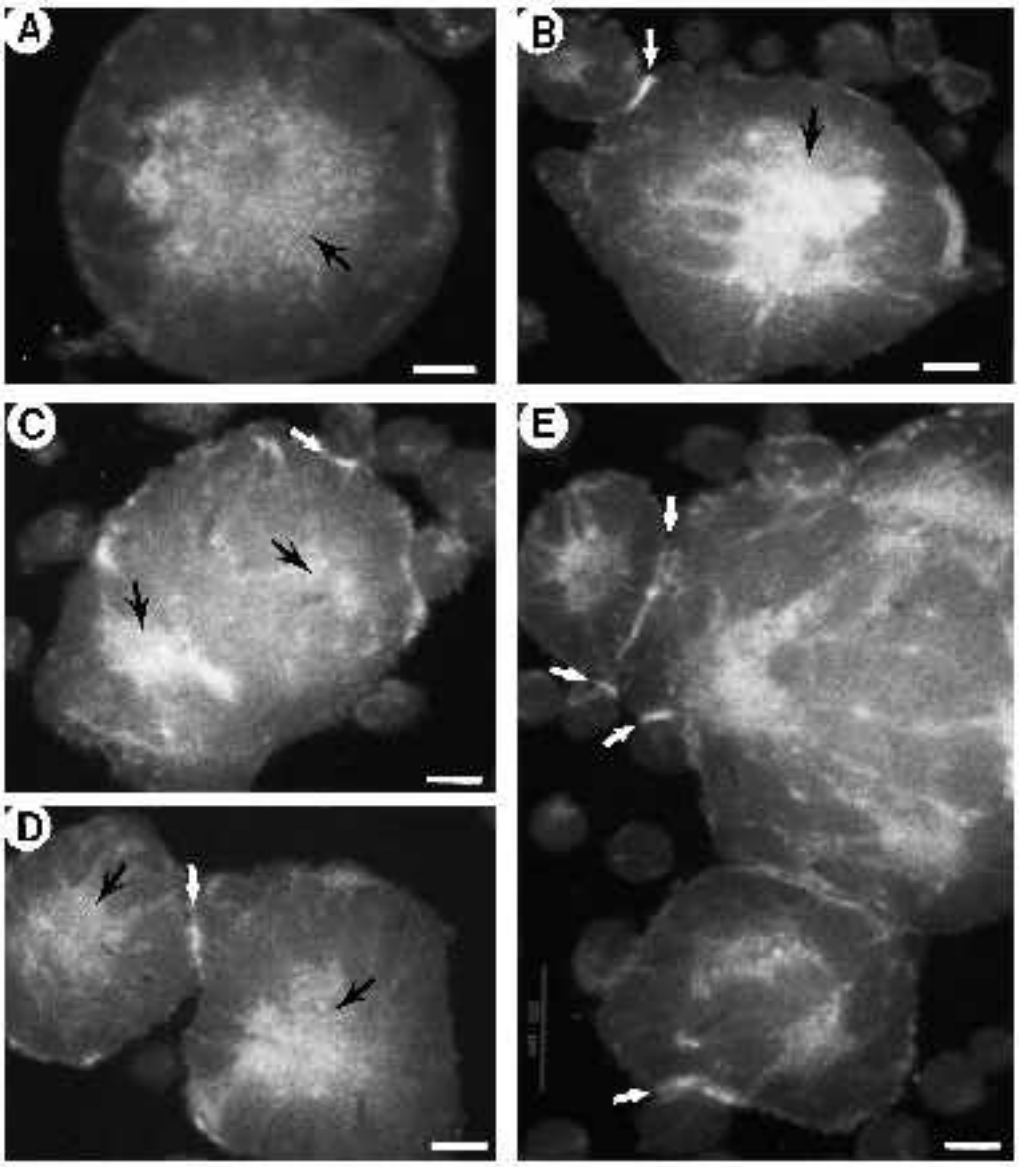

Fig. 7. The distribution of F-actin in syncytia. Syncytia were stained with FITC-phalloidin and viewed through a confocal microscope. Note the condensation of F-actin at adhesion sites between single cells and syncytia (pointed to with white arrows in (C) and (E)) and at the adhesion sites between syncytia (pointed to with white arrows in (B),(D) and (E)). Note also the heavy, punctate staining of F-actin in the cores of the blastula-like nuclear balls, most notable in (A) (black arrow), and the lighter staining in the creases of the nuclear lobes and the syncytium cortex. Bars, 10 μm.

persistence of syncytium translocation is demonstrated in the perimeter tracks in Fig. 8A and centroid tracks in Fig. 8B for 3 representative syncytia. Just as in the case of single cell translocation (Fig. 4A and B), there are long stretches of relatively linear translocation with little lateral derivations for all 3 syncytia. This is supported by the directionality and size of the expansion zones (filled) and the direction of the translocation vectors in the difference pictures of representative syncytia 1 and 2 (Fig. 8C and D).

F-actin localization at the site of single cell-syncytium and syncytium-syncytium adhesion

In the process of syncytium development, single cells fuse with each other, single cells fuse with syncytia and syncytia fuse with syncytia. In most cases in which single cells were firmly bound to syncytia or in which small syncytia were firmly bound to large syncytia, phalloidin staining demonstrated F-actin localization at the site of adhesion in the syncytium and/or in the cell. In Fig. 7C,E, examples are presented of F-actin condensation (white arrows) at sites of single cell-syncytium adhesion, and in Fig. 7B,D,E, at sites of syncytium-syncytium adhesion.

Movement of single cells into syncytia

The high level of motility of both individual cells and syncytia suggested that cell-cell, cell-syncytium and syncytium-syncytium adhesion and subsequent fusion is initiated by dynamic cell contacts. In addition, the fact that both pseudopods and adhesion sites are enriched in F-actin suggested that pseudopod extension from either individual cells or syncytia may be involved in the adhesion-fusion process. In several cases, cells within a cell diameter of the syncytium perimeter were drawn to the syncytium by small pseudopodial projections emanating from the syncytium. In other cases, cells extended a pseudopod towards the syncytium, contacted it, then contracted, drawing the cell body to the syncytium. An example of this latter behavior is presented in a video sequence in Fig. 9. In this sequence, the single cell in the lower right hand corner of the panel extends a pseudopod towards the syncytium above it

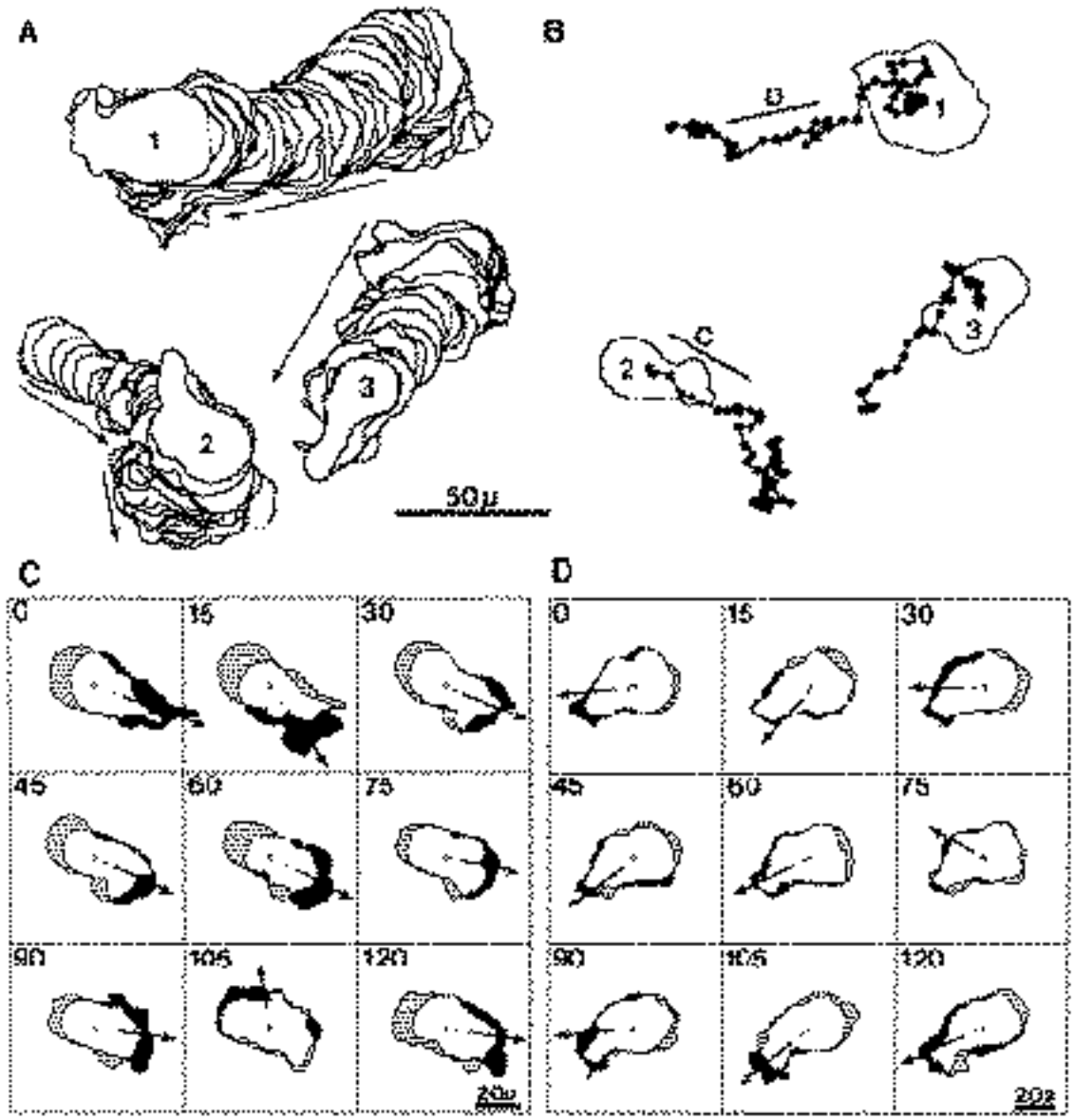

Fig. 8. Motility of syncytia. Syncytia were videorecorded and digitized into the DIAS data file. Tracks of syncytium perimeters (A) and syncytium centroids (B) were then computer-generated and plotted at 15 second intervals. Arrows point in the direction of translocation for the cells in (A). The syncytium perimeter is presented at zero time in the centroid plots in (B). Difference pictures were generated in (C) and (D) for syncytia 1 and 2 in which expansion zones are filled, contraction zones are hatched and common are unfilled. The interval between the 2 images in each difference picture was 15 seconds. The direction of translocation is noted by an arrow in each difference picture. The periods during which the difference pictures were generated in (C) and (D) are diagrammed as lines in (B). μ represents μm.

between 0 and 20 seconds. The pseudopod contacts the syncytium at 60 seconds. Between 60 and 110 seconds, the length of the pseudopod and the position of the cell body remain relatively fixed. However, between 110 and 140 seconds, the pseudopod contracts, drawing the cell body to the syncytium. Between 140 and 160 seconds, a tight contact is formed between the cell body and syncytium.

DISCUSSION

In AIDS patients, there is a decline in CD4-positive T cells, which results in opportunistic infections (Redfield and Burke, 1988). Surprisingly, only a fraction of CD4-positive T cells in AIDS patients are productively infected with HIV (Harper et al., 1986; Simmonds et al., 1990), and it is still not clear how this T cell population is diminished during the course of the disease. Two different mechanisms have been proposed to account for HIV-induced T cell death, syncytium formation through induced cell fusions (Sodroski et al., 1986) and syncytium-independent cell killing (Somasundaran and Robinson, 1987; Leonard et al., 1988). Recently, the capacity of HIV to induce syncytium formation in vitro has been demonstrated to reflect an increase in the virulence of the HIV virus-associated with progression of AIDS (Cheng-Mayer et al., 1988; Tersmette et al.,

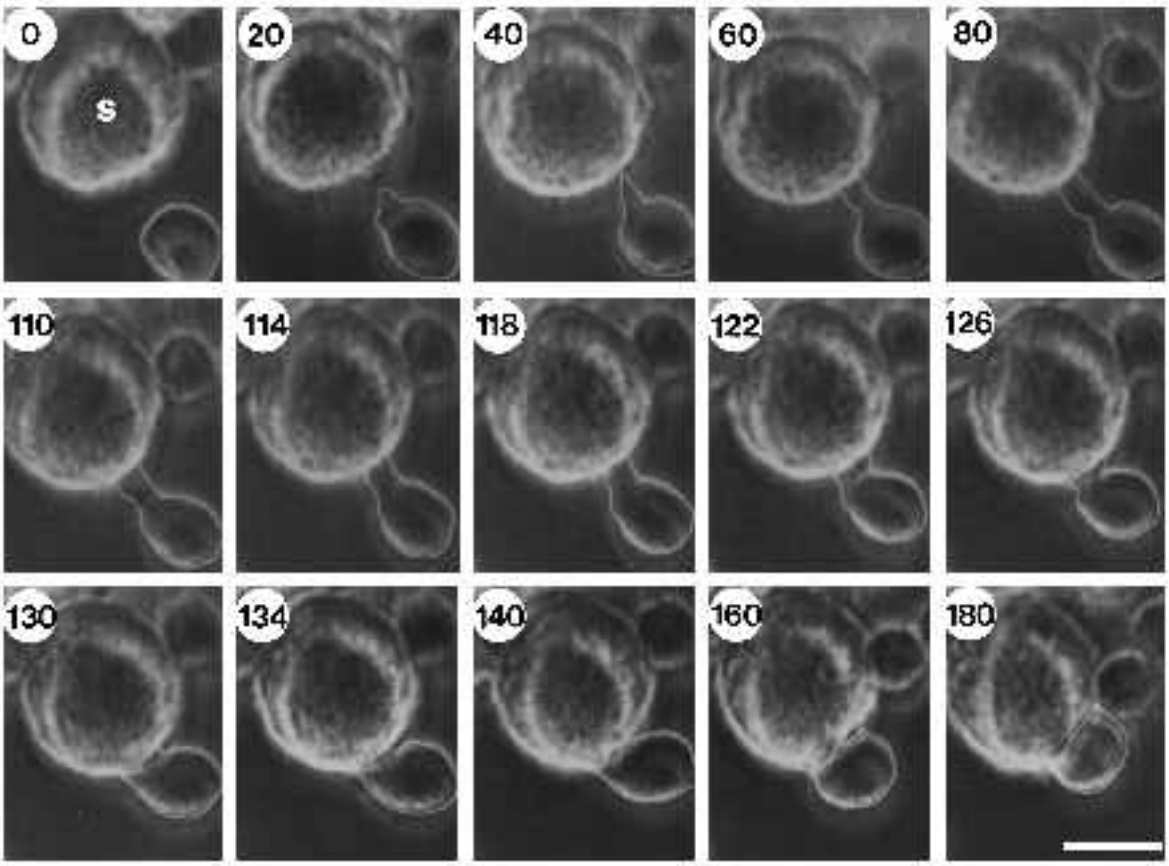

Fig. 9. The involvement of pseudopod extension in the migration of a single cell to a syncytium surface. A field containing a syncytium and a single cell within 15 um of the syncytium perimeter was video recorded, the videorecording was frame-grabbed into the DIAS data file, and the perimeter of the single cell was outlined in white in the digitized images using the manual digitizing option of DIAS. The digitized images with outlines were rephotographed from the monitor screen. Time, in the upper left hand corner of each panel, is presented in seconds. Note that the period of time between contact of the pseudopod and the syncytium perimeter (60 seconds) and the time of nearly complete pseudopod contraction (126 seconds) was roughly 1 minute. Bar in panel 180 represents 15 μm.

1989), and syncytia have been observed in vivo (Gendelman et al., 1988; Koeing et al., 1986).

In spite of its potential role in cytopathogenesis in vivo (Lifson et al., 1986a; Sodroski et al., 1986) and its use as an in vitro indicator of in vivo virulence of the virus (Cheng-Mayer et al., 1988; Tersmette et al., 1989), there has been very little attention paid to the behavioral consequences of HIV-infection in individual T cells or to the behavioral consequences of the HIV-induced fusion events leading to syncytium formation. There seem to be a number of reasons for this lack of attention. First, there have been surprisingly few studies reported on the behavior and cytoskeletal organization of uninfected CD4-positive T cells. Second, it has been assumed that HIV-induced syncytia are relatively inert and disorganized products of fusion. Third, cell interactions leading to fusion have been assumed to be dependent simply on the interaction of the CD4 receptor and the virally encoded gp120 protein inserted into the plasma membrane of infected cells (Lifson et al., 1986; Sodroski et al., 1986; Camerini and Seed, 1990; Ashorn et al., 1990; Broder and Berger, 1993). Based upon the assumption that cell-cell, cell-syncytium and syncytium-syncytium fusions may depend upon cell and syncytium motility, pseudopod extension and the dynamic reorganization of the cytoskeleton, we have begun to analyze the behavior of single cells and syncytia, and the organization of the cytoskeleton during HIV-induced syncytium formation in the CD4-positive T cell line SupT1. We have found that small, medium and large syncytia (containing over 100 nuclei) attempt to maintain the polar organization of a single T cell. Most syncytia form a single dominant pseudopod, thus defining their anterior ends. In addition, syncytia organize nuclei and cytoskeleton into a pattern consistent with the subcellular organization of a mononucleate SupT1 cell. Instead of random distribution, the nuclei of medium sized syncytia (e.g. ones containing approximately 10 to 25 nuclei) are organized into blastula-like balls with nuclear-free cores. This organization generates a relatively round morphology similar to that of individual T cells. In addition, the microtubule organizing centers appear to be located on the peripheral surfaces of nuclei (D. Wessels, S. Anderson, R. Warren, D. Soll and R. Kennedy, unpublished observations), creating a microtubule array around the blastula-like nuclear ball, which is analogous to the microtubule array around a single nucleus in an individual cell. The core of the blastula-like nuclear complex is filled with F-actin, staining in a punctate fashion similar to the condensation of punctate F-actin in single cells. This may represent ves-

icle localization at the Golgi. In addition, F-actin stains lightly under the plasma membrane of the main syncytium body and more intensely in the giant pseudopod. Therefore, syncytia one to two orders of magnitude greater in volume than a single cell mimic the polar integrity of a single motile T cell. In very large syncytia, which appear to have evolved from syncytium-syncytium fusions, the original blastula-like nuclear complexes of the fusing syncytia maintain their original organization, resulting in single membrane-bound large syncytia with multiple nuclear complexes, each with a nuclear free core enriched with F-actin. Even these latter giant fusion products tend to form a giant pseudopod in a polar fashion.

The polar extension of a single pseudopod and organized subcellular architecture are requisites for persistent cellular translocation of many cell types (Trinkaus, 1984). These same cellular characteristics are expressed by multinucleate syncytia, and it may, therefore, be no surprise that they are capable of translocation. HIV-induced syncytia can extend one large anterior pseudopod as well as smaller surface protrusions. They continuously change shape, and they can translocate. In fact, translocating syncytia move with velocities similar to that of individual SupT1 cells on plastic, and with the same level of directionality. How effective the motile behaviors are of HIV-induced syncytia on a more natural substratum than the plastic wall of a tissue culture flask is now being tested, and the possible role of motile HIV-induced syncytia in vivo remains speculative. However, our results lay to rest the perception that HIV-induced syncytia are relatively inert, disorganized cell fusion products and that fusion is a result of passive cellular collisions.

It was previously demonstrated that polyethylene glycol-induced syncytia of baby hamster kidney fibroblast cells (BHK cells) are capable of generating polarity and translocating (Lewis and Albrecht-Buehler, 1987; Lewis-Alberti, 1989). Fusion of BHK cells results in nuclear clustering in the cell center and colocalization of multiple microtubule organizing centers. Just as in the case of SupT1, BHK syncytia reorganize their cytoskeleton and position their nuclei in order to mimic the organization of the single cell of origin. However, the mimicry observed in BHK syncytia involves genesis of a different subcellular morphology in which small nuclei cluster, but not in a blastula-like complex, in order to generate the spread morphology of a fibroblast.

We have also found that small pseudopods projecting from HIV-induced syncytia as well as pseudopods emanating from single SupT1 cells can play an active role in bringing syncytia and single cells together in culture for the fusion event. The F-actin condensations at adhesion sites may represent the remnants of the F-actin in pseudopods, which was involved in the active recruitment of fusion partners. Alternatively, actin may polymerize at adhesion sites after recruitment and may play a crucial role in the adhesion and/or fusion process itself.

In conclusion, our results demonstrate that both single SupT1 cells and HIV-induced syncytia are motile, and that syncytium formation may therefore involve not only individual T cell motility, but also syncytium motility. In addition, we have found that HIV-induced syncytia are highly organized polar giant cells, capable of extending single giant pseudopods. These behaviors involve dynamic changes in the cytoskeleton, and the fusion event may involve an actin-based process.

This research was supported in part by NIH grant HD-18577 to D.R.S., NIH postdoctoral training grant HD07216, which supported D.W., and grants AI-26462 and AI-28696, and a contract from the US Army Research and Development Command to R.C.K. The authors are indebted to E. Voss for assistance in the computer analysis of behavior, and to M. Solursh, K. Jensen and Karla Daniels for help in some of the studies of uninfected cells carried out at the University of Iowa.

REFERENCES

Ashorn, P. A., Berger, E. A. and Moss, B. (1990). Human immunodeficiency virus envelope glycoprotein/CD4 mediated cell fusion of nonprimate cells with human cells. *J. Virol.* **64**, 2149-2156.

Broder, C. C. and Berger, E. A. (1993). CD4 molecules with a diversity of mutations encompassing the CDR3 region efficiently support human immunodeficiency virus type 1 envelope glycoprotein mediated cell fusion. *J. Virol.* **67**, 913-926.

Camerini, D. and Seed, B. (1990). A CD4 domain important for HIV mediated syncytia formation lies outside the virus binding site. *Cell* **60**, 747-754.

Cheng-Mayer, C., Seto, D., Tateno, M. and Levy, J. A. (1988). Biological features of HIV that correlate with virulence in the host. *Science* **240**, 80-82.

Fauci, A. S. (1988). The human immunodeficiency virus: infectivity and mechanisms of pathogenesis. *Science* **239**, 617-622.

Gendelman, H. E., Leonard, J. M., Dutko, F. J., Kowning, S., Khillan, J. S. and Meltzer, M. S. (1988). Immunopathogenesis of human immonodeficiency virus infection in the central nervous system. *Ann. Neurol.* **23**, S78-S81.

Harper, M. E., Marselle, L. M., Gallo, R. C. and Wong-Staal, F. (1986). Detection of lymphocytes expressing human T-lymphotropic virus type III in lymph nodes and peripheral blood from infected individuals by in situ hybridization. *Proc. Nat. Acad. Sci. USA* **83**, 772-776.

Koeing, S., Gendelman, H. E., Orenstein, J. M., Dal Canto, J. M., Pezeshkpour, G. H., Yungbluth, M., Janotta, F., Aksamit, A., Martin, M. A. and Fauci, A. S. (1986). Detection of AIDS virus in macrophages in brain tissue from AIDS patients with encephalopathy. *Science* **233**, 1089-1093.

Lane, M. C., Depper, J. L., Greene, W. C., Whalen, G., Waldman, T. and Fauci, A. S. (1985). Qualitative analysis of immune function in patients with acquired immunodeficiency syndrome. *New. Engl. J. Med.* **313**, 79-84.

Leonard, R., Zagury, D., Desportes, I., Bernard, J., Zagury, J. F. and Gallo, R. C. (1988). Cytopathic effect of human immunodeficiency virus in T4 cells is linked to the last stage of virus infection. *Proc. Nat. Acad. Sci. USA* **85**, 3570-3574.

Lewis, L. and Albrecht-Buehler, G. (1987). Distribution of multiple centrospheres determines migration of BHK syncytia. *Cell Motil. Cytoskel.* **7**, 282-290.

Lewis-Alberti, L. (1989). Altering the vector of polarity of BHK syncrytia changes their motile behavior. *Cell Motil. Cytoskel.* **14**, 187-193.

Lifson, J. D., Reyes, G. R., McGrath, M. S., Stein, B. S. and Engleman, E. G. (1986a). AIDS retrovirus induced cytopathology: giant cell formation and involvement of CD4 antigen. *Science* **232**, 1123-1127.

Lifson, J. D., Feinberg, M. B., Reyes, G. R., Rabin, L., Banapour, B., Chakrabarti, S., Moss, B., Wong-Staal, F., Steimer, S. and Engleman, E. G. (1986b). Induction of CD4-dependent cell fusion by HTLV-III/LAV envelope glycoprotein. *Nature* **323**, 725-728.

Maron, M. J. (1982). *Numerical Analysis.* Macmillan. New York.

Redfield, R. R. and Burke, D. S. (1988). HIV infection: the clinical picture. *Sci. Amer.* **259**, 90-98.

Simmonds, Balfe, P., Peuthere, J. F., Ludlam, C. A., Bishop, J. O. and Brown, A. J. (1990). Human immunodeficiency virus-infected individuals contain provirus in small numbers of peripheral mononuclear cells and at low copy numbers. *J. Virol.* **64**, 864-872.

Smith, S. D., Shatsky, M., Cohen, P. S., Warake, R., Link, M. P. and Glader, B. E. (1984). Monoclonal antibody and enzymatic profiles of human malignant T lymphoid cells and derived cell lines. *Cancer Res.* **44**, 5657-5660.

Sodroski, J., Goh, W. C., Rosen, C., Campbell, C. and Haseltine, W. (1986). Role of the HTLV-III/LAV envelope in syncytium formation and cytopathicity. *Nature* **322**, 470-474.

Somasundaran, M. and Robinson, H. L. (1987). A major mechanism of human immunodeficiency virus induced cell killing does not involve cell fusion. *J. Virol.* **61**, 3114-3119.

Soll, D. R. (1988). 'DMS', a computer-assisted system for quantitating motility, the dynamics of cytopathic flow and pseudopod formation: its application to *Dictyostelium* chemotaxis. *Cell Motil. Cytoskel.* (Suppl.) **10**, 91-106.

Soll, D. R., Voss, E., Varnum-Finney, B. and Wessels, D. (1988). The 'Dynamic Morphology System': a method for quantitating changes in shape, pseudopod formation, and motion in normal and mutant amoebae of *Dictyostelium discoideum. J. Cell. Biochem.* **37**, 177-192.

Tersmette, M., Gruters, R. A., Dewolf, F., DeGoede, R. E. Y., Lange, J. M. A., Schelekens, P. T. A., Goudsmit, J., Huisman, H. G. and Miedema, F. (1989). Evidence for a role of virulent human immunodeficiency virus (HIV) variants in the pathogenesis of AIDS: Studies on sequential HIV isolates. *J. Virol.* **63**, 2118-2125.

Titus, M. A., Wessels, D., Spudich, J. A. and Soll, D. (1993). The unconventional myosin encoded by the myo A gene plays a role in *Dictyostelium* motility. *Mol. Biol. Cell* **4**, 233-246.

Trinkaus, J. P. (1984). *Cells Into Organs: The Forces That Shape The Embryo.* Prentice-Hall, Inc. Englewood, NJ.

Wessels, D. and Soll, D. R. (1990). Mysoin II heavy chain null mutant of *Dictyostelium* exhibits defective intracellular particle movement. *J. Cell. Biol.* **111**, 1137-1148.

(Received 21 June 1993 - Accepted 13 August 1993)